THE JOURNAL OF PHYSICAL CHEMISTRY Letters

Letter

pubs.acs.org/JPCL

Excitation Wavelength Dependence of the Dynamics of Bimolecular Photoinduced Electron Transfer Reactions

Romain Letrun and Eric Vauthey*

Department of Physical Chemistry, University of Geneva, 30 quai Ernest-Ansermet, CH-1211 Geneva 4, Switzerland

Supporting Information

ABSTRACT: The dynamics of photoinduced electron transfer between polar acceptors and donors has been investigated in apolar solvents using femtosecond-resolved fluorescence spectroscopy. It was found to be ultrafast and to continuously accelerate by varying the excitation wavelength from the maximum to the red edge of the absorption band of the acceptor, the overall difference being as large as a factor 4−5. This violation of the Kasha−Vavilov rule is explained by a correlation between the composition of the acceptor environment and its transition energy, that is, the more donors around an acceptor, the longer its absorption wavelength, and the faster the quenching. Because of preferential solvation, this dependence is already observed at low quencher concentrations. This effect, which requires quenching to be faster than the fluctuations of the environment composition, should be quite general for photoinduced charge transfer processes in low-polarity, viscous, or rigid media, such as those used in organic optoelectronic devices.

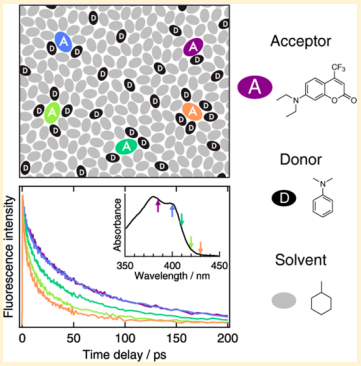

SECTION: Spectroscopy, Photochemistry, and Excited States

Electronic coupling and solvation play a key role in the dynamics of electron transfer (ET) processes.[1−6] In terms of Marcus theory, the coupling impacts the probability of barrier crossing, whereas solvation influences the energetics and the height of the activation barrier.[1] In most cases, these two parameters are unrelated, the first depending mostly on the distance and mutual orientation of the reactants and the second on the dielectric properties of the environment. However, electronic coupling and solvation are interrelated if one of the reactants also acts as solvent or constitutes the major part of the environment. This case has been considered by several groups, who investigated ET fluorescence quenching of various electron-accepting fluorophores in electron-donating solvents, such as *N*,*N*-dimethylaniline (DMA).[7−13] Molecular dynamics simulations by Castner and co-workers showed that, among the ca. 15 DMA molecules surrounding a coumarin, at least 2−5 are, at a given instant, at a proper orientation and distance to result in a large overall electronic coupling between fluorophore and quencher and, thus, in an ET faster than further reorganization of the environment.[11] Investigations from our group on the ET fluorescence quenching of perylene derivatives in DMA additionally pointed out the importance of nonspecific interactions between the reactants.[14,15] The faster quenching dynamics measured with 3-cyanoperylene (PECN) compared to perylene (PE) was shown to be due to dipole−dipole interactions that lead to a preorientation of the reactant pairs and a more favorable electronic coupling. In such a case, electronic coupling and solvation are strongly connected.

We report here on our investigation of the ET fluorescence quenching of coumarins and perylenes by anilines in apolar solvents (Chart 1), aiming at further exploring this relation between coupling and solvation. Coumarins are well-known solvatochromic probes because of their substantial polarity in the electronic ground state and large increase of dipole moment upon excitation to the S_1 state.[16,17] The reason for using polar electron donors and apolar solvents is to introduce a correlation between the $S_1 \leftarrow S_0$ transition energy of the acceptor and the presence of donors in its close environment. In other words, acceptors surrounded by polar donors should absorb at longer wavelength than those with only apolar solvent around them and should, thus, undergo faster ET quenching. This idea is related to the so-called red-edge effect observed with similarly polar molecules in rigid or slow relaxing polar media.[18−26] In such cases, the absorption spectrum is inhomogeneously broadened and, as a consequence, properties such as the fluorescence spectrum and lifetime depend on the excitation wavelength.[18−26] This effect is mostly observed on the red side of the absorption band where only the 0−0 transition is excited. However, to the best of our knowledge, red-edge effects on photoinduced ET dynamics have not been reported so far. We will show that the ET dynamics can vary by a factor as large as 4−5 when increasing the excitation wavelength. These results should also be relevant to ET processes in rigid media, such as those used in organic optoelectronic devices.[27−29]

The absorption spectra of the acceptors in methylcyclohexane (MCH) alone and with 0.5 M DMA are depicted in Figure 1 and Supporting Information Figures S1 and S2, whereas the effect of increasing DMA concentration is shown in Supporting Information Figure S3. With the nonpolar PE, the presence of

Received: March 20, 2014
Accepted: April 25, 2014
Published: April 25, 2014

dx.doi.org/10.1021/jz500569r | J. Phys. Chem. Lett. 2014, 5, 1685−1690

Chart 1. Structure and Properties of the Acceptors, Donors, and Solvents[a]

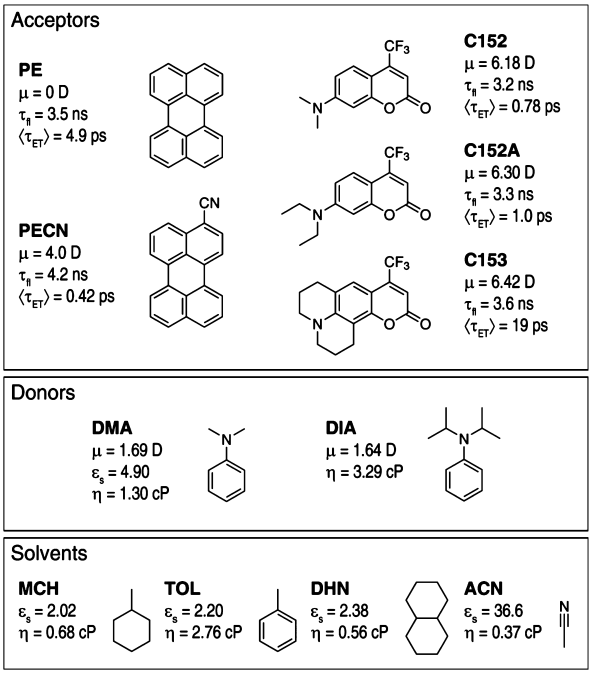

[a] μ, electric dipole moment (from AM1 calculations); τ_{fl}, fluorescence lifetime in MCH; $\langle\tau_{ET}\rangle$, average quenching time constant in DMA;[14,30] ε_s, static dielectric constant;[31] η, viscosity.[31]

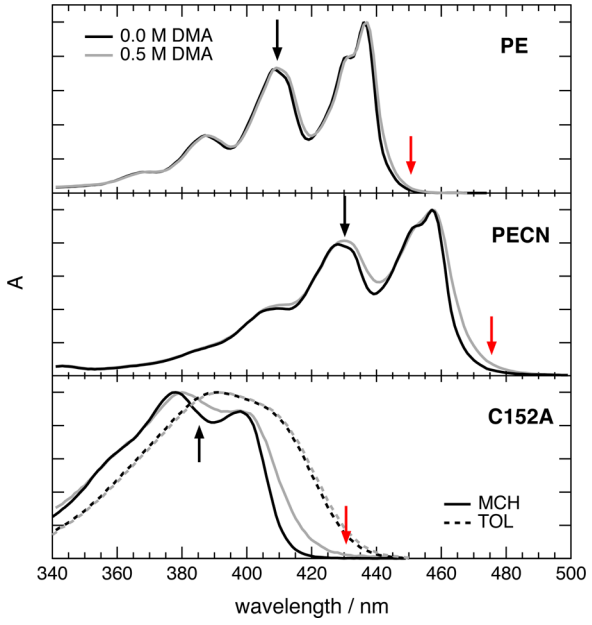

Figure 1. Absorption spectra of PE, PECN, and C152A in MCH (solid lines) and TOL (dashed lines) with and without 0.5 M DMA. The arrows indicate the excitation wavelengths used for the time-resolved fluorescence measurements shown in Figure 3.

DMA results in a minor bathochromic shift (~50 cm^{-1}), which can be accounted for by the change of refractive index.[32] With the mildly polar PECN, a broadening of the red wing of the band can additionally be observed. Finally, with the most polar acceptors, coumarins, both the shift and the broadening are more pronounced. These effects disappear in the aromatic toluene (TOL), the spectra being independent of the presence of DMA. In MCH, the red-side band broadening can be explained by the large variety of local environments around the acceptors, that is, of the solvation energies and, thus, of $S_1 \leftarrow S_0$ transition energies, introduced by the dipole−dipole interaction with the polar DMA. This interaction should also lead to a dielectric enrichment or preferential solvation effect,[33,34] that is, to a larger concentration of DMA around the polar acceptor than in the bulk solution.

In TOL, $\pi-\pi$ as well as quadrupolar interactions with the acceptor should be of a similar order of magnitude as the interactions with DMA,[35] and thus, the band broadening relative to MCH should arise from the distribution of arrangements of TOL around the acceptor. The presence of DMA around the acceptor does apparently not increase the solvation energy very significantly. As a consequence, the dielectric enrichment effect in TOL can be expected to be substantially smaller than in MCH.

Finally, the smaller effect observed with PECN compared to the coumarins can be accounted for by its weaker polarity and the smaller difference of dipole moment between ground and excited state, that is, by the smaller solvatochromism of its absorption band.[14]

The fluorescence quantum yields in the presence of 0.5 M DMA are generally extremely weak, and reliable steady-state spectra could only be recorded with C153, for which the quenching is somewhat slower. Whereas the fluorescence spectrum of C153 in pure MCH is structured and independent of the excitation wavelength, it is structureless and shifts and broadens with increasing excitation wavelength upon addition of 0.5 M DMA (Figure 2A). In the latter case, the excitation spectrum recorded upon monitoring at increasing fluorescence wavelength changes progressively from a spectrum that resembles the absorption spectrum in pure MCH to one that is similar to the absorption spectrum with 0.5 M DMA. This is

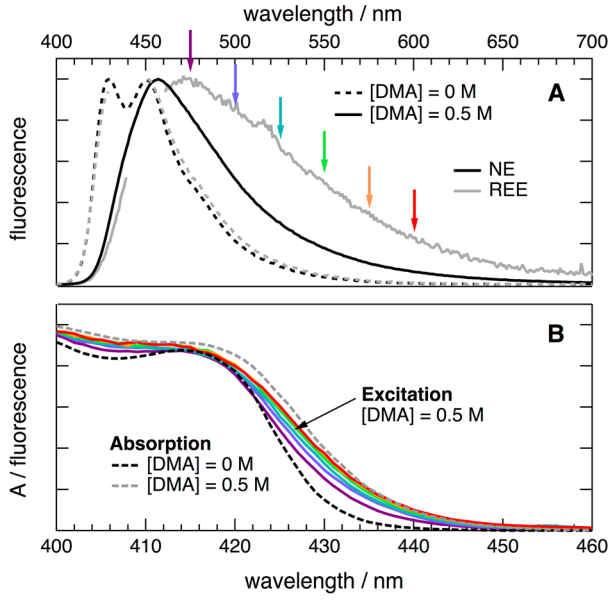

Figure 2. (A) Fluorescence emission spectra recorded using normal (NE, λ_{ex} = 380 nm) and red-edge excitation (REE, λ_{ex} = 440) with C153 in MCH with and without 0.5 M DMA; (B) Fluorescence excitation spectra recorded at the wavelengths indicated by arrows in (A) with C153 in MCH and 0.5 M DMA. The absorption spectra of C153 in MCH with and without 0.5 M DMA are shown for comparison.

dx.doi.org/10.1021/jz500569r | J. Phys. Chem. Lett. 2014, 5, 1685−1690

consistent with the inhomogeneous character of the absorption band: molecules absorbing at long wavelength are in an environment that is more polar than those absorbing at short wavelength and, consequently, have a red-shifted emission spectrum. Therefore, distinct acceptors subensembles with different amounts of DMA in their surrounding can be selectively probed by tuning the excitation wavelength across the red side of the absorption band. This is no longer possible on the blue side of the absorption band, where vibronic transitions take place. In this case, molecules with different 0−0 transition energies can be simultaneously excited to various vibrational excited states. To be observed, this wavelength effect requires excitation to be performed in the 0−0 transition and the excited-state decay of the acceptor to be faster than the fluctuations of its environment.

Fluorescence time profiles measured with the different acceptors and 0.5 M DMA in MCH using the fluorescence up-conversion setup described in refs 36 and 37 are shown in Figure 3 and Supporting Information Figures S1 and S2. With

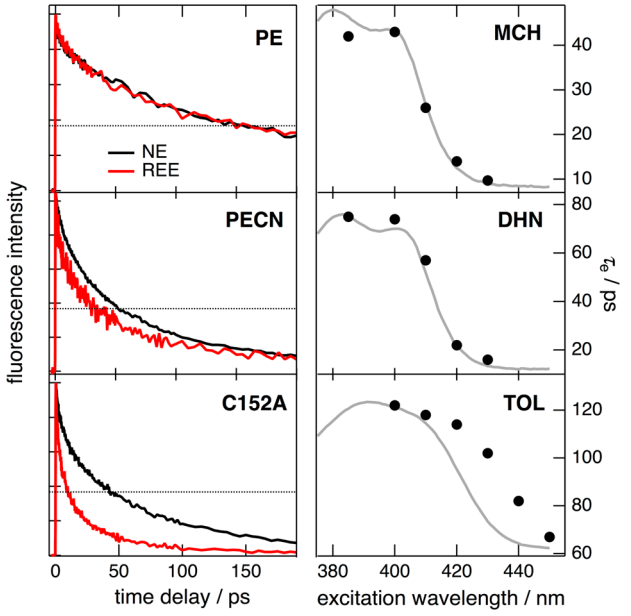

Figure 3. (Left) Time profile of the fluorescence intensity measured at 495 nm with PE and PECN and at 470 nm with C152 in MCH and 0.5 M DMA upon normal and red-edge excitation (arrows in Figure 1, the dotted lines are located at $1/e$ of the initial intensity). (Right) Excitation wavelength dependence of the $1/e$ time constant, τ_e, measured with C152A and 0.5 M DMA in MCH, DHN, and TOL (for comparison the absorption spectra are shown in gray).

all acceptors, except the nonpolar PE, the dynamics recorded upon red-most excitation (red-edge excitation, REE) are markedly faster than those measured when exciting close to the absorption maximum (normal excitation, NE), the effect increasing with the polarity of the acceptor, as is also found for the broadening of the absorption spectrum. Measurements at intermediate excitation wavelengths (Supporting Information Figure S4) reveal that this dependence exists over the entire red side of the absorption band, becoming more pronounced further to the red. The effect vanishes at short wavelengths, where vibronic transitions take place.

This excitation wavelength effect is absent in pure MCH (Supporting Information Figure S5) and, therefore, does not arise from vibrational relaxation following excitation with various amounts of excess energy.[38,39] Similarly, contribution from a dynamic Stokes shift due to the dielectric relaxation with DMA can be ruled out, as the time profiles measured with C152 and 0.5 M DMA in MCH at several wavelengths between 450 and 500 nm do not differ significantly (Supporting Information Figure S6). Therefore, most of the excited-state population decays on a shorter time scale than the fluctuations of the composition of the environment. Finally, the initial fluorescence anisotropy amounts to 0.38, independently of the excitation wavelength (Supporting Information Figure S7), ruling out an excitation of a donor−acceptor complex at long wavelength.

The time profiles were analyzed using the convolution of a Gaussian function, representing the instrument response function, and a sum of exponentials, yielding sets of time constants, τ_i, and amplitudes, α_i. Three to four exponential functions were required to correctly reproduce the data. As similar time constants were obtained for a given acceptor and DMA concentration but different excitation wavelengths, these data sets were analyzed globally. The best-fit parameters obtained for C152A and 0.5 M DMA in MCH, DHN, and TOL are collected in Supporting Information Table S1. In all solvents, the shortest time constant, τ_1, is between 1.4 and 1.8 ps and close to the average ET time, $\langle\tau_{ET}\rangle$ = 1.0 ps, reported by Shirota et al. in pure DMA.[40] Furthermore, the amplitude of this component increases by a factor of about 2 by going from 385 to 430 nm excitation. This time constant is much shorter than that expected for a diffusional quenching and, thus, can be attributed to the static quenching by the donor molecules located in the close proximity of the acceptor and that do not need to diffuse for undergoing ET. This indicates that (i) because the concentration of pure DMA is 7.9 M, the local DMA concentration around the acceptors undergoing this fast decay is probably larger than the bulk concentration of 0.5 M, pointing to substantial dielectric enrichment and (ii) this acceptor subpopulation absorbs preferentially at long wavelengths, that is, on the red edge of the ensemble absorption band. The slower components of the decay can be attributed to the transient and stationary stages of the quenching.[41] A proper description of the whole fluorescence decay would require a model, such as differential encounter theory,[42,43] that takes all these stages of the quenching into account. However, these models cannot be readily used here as the reactant-pair distribution function depends on the excitation wavelength.

The dynamics being highly nonexponential, it is useful to have a characteristic time for comparing them and quantifying the effect of the excitation wavelength. One can use either the initial time constant, τ_0, that corresponds to the inverse of the slope at time zero, the amplitude-averaged time constant, $\langle\tau\rangle$, or the time, τ_e, after which the fluorescence intensity has decayed from its initial value, I_0, to I_0/e. Whereas τ_0 and $\langle\tau\rangle$ put more emphasis on the short and long time behaviors, respectively, τ_e gives a good description of the overall time scale of the decay and, thus, will be used further on. The τ_e values obtained for C152A with 0.5 M DMA in MCH, DHN, and TOL are plotted as a function of the excitation wavelength in Figure 3 and listed in Supporting Information Table S1. In all three solvents, τ_e remains essentially constant upon excitation around the maximum of the absorption band but decreases dramatically with increasing wavelength. The magnitude of this effect was quantified by taking the ratio of the τ_e values measured upon normal and red-edge excitation, τ_e^{NE}/τ_e^{REE}. This ratio amounts to 4−5 in the nonaromatic

dx.doi.org/10.1021/jz500569r | J. Phys. Chem. Lett. 2014, 5, 1685−1690

solvents, MCH and DHN, whereas it is only around 2 in TOL. This is most probably due to the aromatic nature of TOL, as discussed above. In this solvent, the correlation between the local DMA concentration and the transition energy of the acceptor is attenuated by the $\pi-\pi$ and quadrupolar interactions with the solvent. The slower quenching in TOL by a factor 2–4, depending on the excitation wavelength (Supporting Information Table S1), probably arises from a lower local concentration of DMA due to a weaker dielectric enrichment. This effect is even stronger in ACN, where the quenching dynamics of C152A by 0.5 M DMA is also slower than in apolar solvents and is independent of the excitation wavelength (Supporting Information Figure S8 and Table S3). In this case, preferential solvation favors ACN and no longer DMA. Furthermore, the presence of DMA around the acceptor has essentially no effect on its solvation energy and, thus, on its $S_1 \leftarrow S_0$ transition energy.

The excitation wavelength effect was also investigated as a function of DMA concentration. As shown in Figure 4A, the

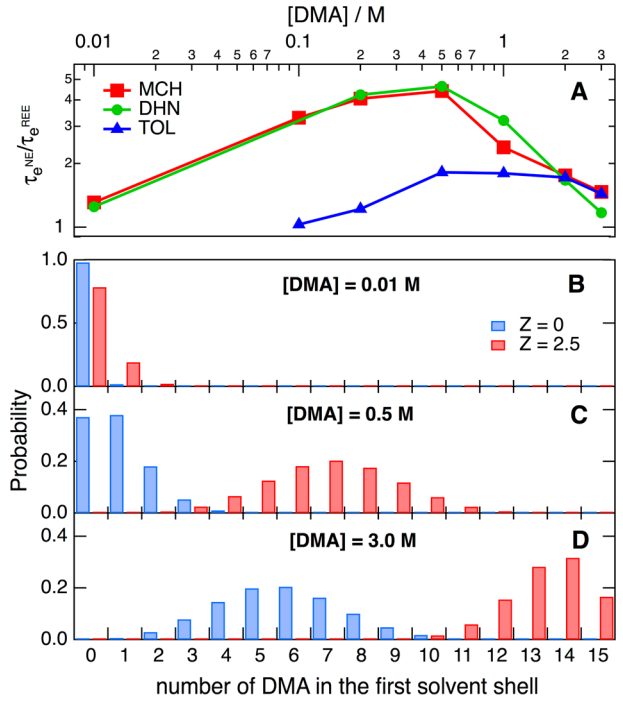

Figure 4. (A) Dependence of the excitation wavelength effect quantified by the τ_e^{NE}/τ_e^{REE} ratio on the DMA concentration. (B–D) Probability to find n DMA molecules in the first solvent shell of the acceptor at different bulk concentrations of quencher without ($Z = 0$) and with ($Z = 2.5$) preferential solvation.

effect in nonaromatic solvents is already present at 0.01 M DMA, the smallest concentration investigated, and only appears above 0.1 M in TOL. This further confirms the large effect of DMA on the solvation energy in MCH and DHN and the existence of a dielectric enrichment. In all solvents, the plot of the τ_e^{NE}/τ_e^{REE} ratio vs DMA concentration exhibits first a rise up to ca. 0.5 M and then a decay at higher quencher concentrations. This dependence reflects the width of the distribution of local environments. At low concentrations, acceptors are either surrounded by solvent only or by at most one molecule of DMA, leading to a small inhomogeneous broadening. The situation is similar, but reversed, at high DMA concentrations, where all acceptors have many DMA molecules in their vicinity and are all well solvated. The largest variety of local environments, and consequently the largest inhomogeneous broadening, is found at intermediate concentrations.

The probability density function (PDF) describing the probability to find n molecules of DMA in the first solvent shell of an acceptor is given by a simple binomial distribution[44]

$$f_{N,p}(n) = \frac{N!}{(N-n)!n!}p^n(1-p)^{N-n} \quad (1)$$

where N is the total number of sites around an acceptor and p the probability for a molecule to be a donor and not a nonreacting solvent molecule. Figure 4B–D shows PDFs evaluated for three bulk concentrations of DMA assuming $N = 15$ and taking the mole fraction of DMA for p. The inhomogeneity of the environments is very small at the lowest concentration and increases substantially at 0.5 M. However, contrary to what could be expected from Figure 4A, it does not decrease when going to 3 M.

These calculations do not take preferential solvation into account and assume that the DMA concentration around the acceptors is the same as the bulk concentration. According to Suppan's model of the dielectric enrichment,[33] the ratio of the mole fractions of the polar, P, and nonpolar constituents, N, around the acceptor, y_P and y_N, is related to the ratio of bulk mole fractions, x_P and x_N, via the preferential solvation index, Z

$$\frac{y_N}{y_P} = \frac{x_N}{x_P}e^{-Z} \quad \text{with} \quad Z = \frac{3M\mu^2\Delta f(\varepsilon)_{N,P}}{32\pi^2\varepsilon_0\delta RTr^6} \quad (2)$$

where M is the average molecular weight of N and P, μ the dipole moment of the acceptor, $\Delta f(\varepsilon)_{N,P}$ the difference between the Onsager functions of N and P, δ the average density of N and P, r the radius of the acceptor, and ε_0, R, and T have their usual meaning. A value of $Z = 2.5$ has been estimated for C152A with P = DMA, N = MCH, and the parameters listed in Supporting Information Table S2. Figure 4B–D shows that the PDFs for 0.01 and 0.5 M DMA calculated with the local mole fraction of DMA, that is, with $p = y_P$, are substantially broader than without taking preferential solvation into account. On the other hand, the PDF narrows at 3 M DMA due to a saturation of the number of DMA molecules surrounding the acceptors. Although the model is rather crude, it qualitatively reproduces the experimentally observed trend (Figure 4A).

The wavelength effect reported here is a direct consequence of a correlation between the electronic coupling of the reactants and solvation. In the present case, the best solvated acceptors are those undergoing the fastest ET not only because of a larger effective driving force but also because of a larger overall coupling between the acceptor and the surrounding quencher molecules. This wavelength excitation effect does not require exceptional conditions to be observed. The necessary ingredients are (i) a molecule exhibiting solvatochromism in absorption, a polar quencher, and an apolar or weakly polar solvent to ensure inhomogeneous broadening of the absorption band, and (ii) ET quenching occurring on a shorter time scale than that of the fluctuations of the environment. This last condition is met here in both MCH and DHN, although the former is 4 times less viscous. Replacing DMA by a weaker quencher, such as DIA, results in ET times smaller by a factor of ca. 2 and a weaker excitation wavelength dependence (Supporting Information Figure S9). With C152A and 0.5 M quencher in MCH, the τ_e^{NE}/τ_e^{REE} ratio decreases from 4.4 with DMA to 2.8 with DIA. Similarly, with DMA but various

dx.doi.org/10.1021/jz500569r | J. Phys. Chem. Lett. 2014, 5, 1685–1690

coumarins, both the ET rate and the τ_e^{NE}/τ_e^{REE} ratio decrease in the order C152 > C152A > C153 (τ_e^{NE}/τ_e^{REE} = 4.6 > 4.4 > 2.2). In viscous and rigid environments, such dependence on the excitation wavelength can be expected even with slower ET processes and should be considered when investigating photoinduced charge transfer dynamics in optoelectronic devices, like those used for solar energy conversion.[27−29]

■ ASSOCIATED CONTENT

Supporting Information

Experimental details; absorption spectra of C152, C152A, and C153 in MCH with various concentrations of DMA; fluorescence dynamics of C152, C152A, and C153 in MCH with 0.5 M DMA at various excitation wavelengths; fluorescence dynamics of C152A in MCH and ACN at various excitation wavelengths; fluorescence anisotropy; absorption spectra and fluorescence dynamics of C152A in MCH with 0.5 M DIA; best fit parameters obtained from the analysis of the fluorescence dynamics; parameters used for the calculation of the preferential solvation index. This material is available free of charge via the Internet at http://pubs.acs.org.

■ AUTHOR INFORMATION

Corresponding Author

*E. Vauthey. E-mail: eric.vauthey@unige.ch.

Notes

The authors declare no competing financial interest.

■ ACKNOWLEDGMENTS

The authors wish to thank the Fonds National Suisse de la Recherche Scientifique (Project Nr. 200020-147098) as well as the University of Geneva for financial support.

■ REFERENCES

(1) Marcus, R. A.; Sutin, N. Electron Transfer in Chemistry and Biology. *Biochim. Biophys. Acta* **1985**, *811*, 265−322.
(2) Heitele, H. Dynamic Solvent Effects on Electron Transfer Reactions. *Angew. Chem. Int. Ed. Engl.* **1993**, *32*, 359−377.
(3) Bixon, M.; Jortner, J. Electron Transfer: from Isolated Molecules to Biomolecules. *Adv. Chem. Phys.* **1999**, *106*, 35−202.
(4) Liu, M.; Ito, N.; Maroncelli, M.; Waldeck, D. H.; Oliver, A. M.; Paddon-Row, M. N. Solvent Friction Effect on Intramolecular Electron Transfer. *J. Am. Chem. Soc.* **2005**, *127*, 17867−17876.
(5) Wiberg, J.; Guo, L.; Petterson, K.; Nilsson, D.; Ljungdahl, T.; Mårtensson, J.; Albinsson, B. Charge Recombination versus Charge Separation in Donor-Bridge-Acceptor Systems. *J. Am. Chem. Soc.* **2007**, *129*, 155−163.
(6) Rosspeintner, A.; Lang, B.; Vauthey, E. Ultrafast Photochemistry in Liquids. *Annu. Rev. Phys. Chem.* **2013**, *64*, 247−271.
(7) Kandori, H.; Kemnitz, K.; Yoshihara, K. Subpicosecond Transient Absorption Study of Intermolecular Electron Transfer between Solute and Electron-Donating Solvents. *J. Phys. Chem.* **1992**, *96*, 8042−8048.
(8) Nagasawa, Y.; Yartsev, A. P.; Tominaga, K.; Bisht, P. B.; Johnson, A. E.; Yoshihara, K. Dynamical Aspect of Ultrafast Intermolecular Electron Transfer Faster than Solvation Process: Substituent Effects and Energy Gap Dependence. *J. Phys. Chem.* **1995**, *99*, 653.
(9) Wolfseder, B.; Seidner, L.; Domcke, W.; Stock, G.; Seel, M.; Engleitner, S.; Zinth, W. Vibrational Coherence in Ultrafast Electron Transfer Dynamics of Oxazine 1 in *N,N*-Dimethylaniline: Simulation of a Femtosecond Pump-Probe Experiment. *Chem. Phys.* **1998**, *233*, 323−334.
(10) Xu, Q.-H.; Scholes, G. D.; Yang, M.; Fleming, G. R. Probing Solvation and Reaction Coordinates of Ultrafast Photoinduced Electron-Transfer Reactions Using Nonlinear Spectroscopies: Rhodamine 6G in Electron-Donating Solvents. *J. Phys. Chem. A* **1999**, *103*, 10348−10358.
(11) Castner, E. W., Jr.; Kennedy, D.; Cave, R. J. Solvent as Electron Donor: Donor/Acceptor Electronic Coupling is a Dynamical Variable. *J. Phys. Chem. A* **2000**, *104*, 2869−2885.
(12) Morandeira, A.; Fürstenberg, A.; Vauthey, E. Fluorescence Quenching in Electron Donating Solvents. 2. Solvent Dependence and Product Dynamics. *J. Phys. Chem. A* **2004**, *108*, 8190−8200.
(13) Rosspeintner, A.; Angulo, G.; Vauthey, E. Driving Force Dependence of Charge Recombination in Reactive and Nonreactive Solvents. *J. Phys. Chem. A* **2012**, *116*, 9473−9483.
(14) Morandeira, A.; Fürstenberg, A.; Gumy, J.-C.; Vauthey, E. Fluorescence Quenching in Electron Donating Solvents. 1. Influence of the Solute-Solvent Interactions on the Dynamics. *J. Phys. Chem. A* **2003**, *107*, 5375−5383.
(15) Angulo, G.; Cuetos, A.; Rosspeintner, A.; Vauthey, E. Experimental Evidence of the Relevance of Orientational Correlations in Photoinduced Bimolecular Reactions in Solution. *J. Phys. Chem. A* **2013**, *117*, 8814−8825.
(16) Horng, M. L.; Gardecki, J. A.; Papazyan, A.; Maroncelli, M. Subpicosecond Measurements of Polar Solvation Dynamics: Coumarin 153 Revisited. *J. Phys. Chem.* **1995**, *99*, 17311−17337.
(17) R. J. Cave, R. J.; Castner, E. W., Jr. Time-Dependent DFT Investigation of the Ground and Excited States of Coumarins 102, 152, 153 and 343. *J. Phys. Chem. A* **2002**, *106*, 12117−12123.
(18) Galley, W. C.; Purkey, R. M. Role of Heterogeneity of the Solvation Site in Electronic Spectra in Solution. *Proc. Natl. Acad. Sci. U. S. A.* **1970**, *67*, 1116−1121.
(19) Itoh, K. i.; Azumi, T. Shift of the Emission Band upon Excitation at the Long Wavelength Absorption Edge. II. Importance of the Solute−Solvent Interaction and the Solvent Reorientation Relaxation Process. *J. Chem. Phys.* **1975**, *62*, 3431−3438.
(20) Fünfschilling, J.; Zschokke Granacher, I.; Williams, D. F. The Determination of the Site Energy Distribution of Organic Molecules Dissolved in Glassy Matrices. *J. Chem. Phys.* **1981**, *75*, 3669−3673.
(21) Demchenko, A. P. On the Nanosecond Mobility in Proteins: Edge Excitation Fluorescence Red Shift of Protein-Bound 2-(*p*-Toluidinylnaphthalene)-6-Sulfonate. *Biophys. Chem.* **1982**, *15*, 101−109.
(22) Fee, R. S.; Milsom, J. A.; Maroncelli, M. Inhomogeneous Decay Kinetics and Apparent Sdvent Relaxation at Low Temperatures. *J. Phys. Chem.* **1991**, *95*, 5170−5181.
(23) Morgenthaler, M. J. E.; Meech, S. R.; Yoshihara, K. The Inhomogeneous Broadening of the Electronic Spectra of Dyes in Glycerol Solution. A Time Resolved Fluorescence Study. *Chem. Phys. Lett.* **1992**, *197*, 537−541.
(24) Vauthey, E.; Holliday, K.; Wei, C.; Renn, A.; Wild, U. P. Stark Effect and Spectral Hole-Burning: Solvation of Organic Dyes in Polymers. *Chem. Phys.* **1993**, *171*, 253−263.
(25) Mandal, P. K.; Sarkar, M.; Samanta, A. Excitation-Wavelength-Dependent Fluorescence Behavior of Some Dipolar Molecules in Room-Temperature Ionic Liquids. *J. Phys. Chem. A* **2004**, *108*, 9048−9053.
(26) Lakowicz, J. R. *Principles of Fluorescence Spectroscopy*, 3rd ed.; Springer: New York, 2006; p 954.
(27) Köhler, A.; dos Santos, D. A.; Beljonne, D.; Shuai, Z.; Brédas, J.-L.; Holmes, A. B.; Kraus, A.; Müllen, K.; Friend, R. H. Charge Separation in Localized and Delocalized Electronic States in Polymeric Semi-Conductors. *Nature* **1998**, *392*, 903−906.
(28) Offermans, T.; van Hal, P. A.; Meskers, S. S.; Koetse, M. S.; Janssen, R. R. Exciplex Dynamics in a Blend of Pi-Conjugated Polymers with Electron Donating and Accepting Properties: MDMO-PPV and PCNEPV. *Phys. Rev. B* **2005**, *72*, 045213.
(29) Heeger, A. J. A. Semiconducting polymers: the Third Generation. *Chem. Soc. Rev.* **2010**, *39*, 2354−71.
(30) Shirota, H.; Pal, H.; Tominaga, K.; Yoshihara, K. Substituent effect and deuterium isotope effect of ultrafast intermolecular electron transfer: coumarin in electron-donating solvents. *J. Phys. Chem. A* **1998**, *102*, 3089.

(31) Lide, D. R. *Handbook of Chemistry and Physics*, 90th ed.; CRC Press: Boca Raton, FL, 2009.
(32) Suppan, P. Solvatochromic Shifts: the Influence of the Medium on the Energy of Electronic States. *J. Photochem. Photobiol.* **1990**, *A50*, 293−330.
(33) Suppan, P. Local Polarity of Solvent Mixtures in the Field of Electronically Excited Molecules and Exciplexes. *J. Chem. Soc., Faraday Trans. 1* **1987**, *83*, 495−509.
(34) Reichardt, C.; Welton, T. *Solvents and Solvent Effects in Organic Chemistry*, 4th ed.; John Wiley & Sons: Weinheim, Germany, 2011.
(35) Reynolds, L.; Gardecki, J. A.; Frankland, S. J. V.; Horng, M. L.; Maroncelli, M. Dipole Solvation in Nondipolar Solvents: Experimental Studies of Reorganization Energies and Solvation Dynamics. *J. Phys. Chem.* **1996**, *100*, 10337−10354.
(36) Morandeira, A.; Engeli, L.; Vauthey, E. Ultrafast Charge Recombination of Photogenerated Ion Pairs to an Electronic Excited State. *J. Phys. Chem. A* **2002**, *106*, 4833−4837.
(37) Duvanel, G.; Grilj, J.; Chaumeil, H.; Jacques, P.; Vauthey, E. Ultrafast Excited-State Dynamics of a Series of Zwitterionic Pyridinium Phenoxides with Increasing Sterical Hindering. *Photochem. Photobiol. Sci.* **2010**, *9*, 908−915.
(38) Kovalenko, S. A.; Schanz, R.; Hennig, H.; Ernsting, N. P. Cooling Dynamics of an Optically Excited Molecular Probe in Solution from Femtosecond Broadband Transient Absorption Spectroscopy. *J. Chem. Phys.* **2001**, *115*, 3256−3274.
(39) Pigliucci, A.; Duvanel, G.; Daku, L. M. L.; Vauthey, E. Investigation of the Influence of Solute−Solvent Interactions on the Vibrational Energy Relaxation Dynamics of Large Molecules in Liquids'. *J. Phys. Chem. A* **2007**, *111*, 6135−6145.
(40) Shirota, H.; Pal, H.; Tominaga, K.; Yoshihara, K. Substituent Effect and Deuterium Isotope Effect of Ultrafast Intermolecular Electron Transfer: Coumarin in Electron-Donating Solvent. *J. Phys. Chem. A* **1998**, *102*, 3089−3102.
(41) Angulo, G.; Kattnig, D. R.; Rosspeintner, A.; Grampp, G.; Vauthey, E. On the Coherent Description of Diffusion-Influenced Fluorescence Quenching Experiments II: Early Events. *Chem.—Eur. J.* **2010**, *16*, 2291−2299.
(42) Burshtein, A. I. Non-Markovian Theories of Transfer Reactions in Luminescence and Chemiluminescence and Photo-and Electrochemistry. *Adv. Chem. Phys.* **2004**, *129*, 105−418.
(43) Rosspeintner, A.; Angulo, G.; Vauthey, E. Bimolecular Photoinduced Electron Transfer Beyond the Diffusion Limit: The Rehm−Weller Experiment Revisited with Femtosecond Time Resolution. *J. Am. Chem. Soc.* **2014**, *136*, 2026−2032.
(44) Young, H. D. *Statistical Treatment of Experimental Data*; McGraw-Hill: New York, 1962.